

Observing the Meissner effect in neutron stars

S. K. Lander^{1,*}, K. N. Gourgouliatos², Z. Wadiasingh^{3,4,5}, and D. Antonopoulou⁶

¹*School of Engineering, Mathematics and Physics,
University of East Anglia, Norwich, NR4 7TJ, U.K.,*

²*Department of Physics, University of Patras, Patras, Rio, 26504, Greece*

³*Department of Astronomy, University of Maryland, College Park, Maryland 20742, USA,*

⁴*Astrophysics Science Division, NASA Goddard Space Flight Center, Greenbelt, MD 20771, USA,*

⁵*Center for Research and Exploration in Space Science and Technology,
NASA/GSFC, Greenbelt, Maryland 20771, USA, and*

⁶*Jodrell Bank Centre for Astrophysics, Department of Physics and Astronomy, The University of Manchester, UK*

We explore the consequences of a new mechanism for the rapid onset of the Meissner effect in a young neutron star, via an interplay of field-line advection by fluid motion and magnetic reconnection. This mechanism provides the first justification for an assumption at the centre of magnetar simulations. Reconnection leads to a characteristic release of energy, which can be used to constrain superconducting gap models. Our model provides a natural explanation for the recently discovered long-period radio sources, and also has important implications for neutron-star rotational evolution and gravitational-wave emission. The Meissner effect is only operative for field strengths $10^{12} \text{ G} \lesssim B \lesssim 5 \times 10^{14} \text{ G}$.

Introduction. Neutron star (NS) cores host the only known superconductor in the Universe outside terrestrial laboratories [1]. Proton superconductivity does not set in simultaneously across the whole NS core, but rather begins in a thin shell in the star’s outer core which slowly expands both outwards (stopping at the boundary with the crust) and inwards as the star cools, as a result of the strong radial dependence of the critical temperature T_c for superconductivity. If the magnetic field \mathbf{B} threading the NS is weaker than some critical field H_c , the minimum-energy state in the superconducting shell will be dictated by the *Meissner effect*: the expulsion of magnetic flux, leaving $B = 0$ except in a thin surface layer [2]. Whilst on Earth the process is well understood and near-instantaneous, NSs present a different environment: the intense \mathbf{B} (typically $10^{12} - 10^{15} \text{ G}$), is intrinsic to the star and coupled to a highly-conducting fluid of protons and electrons (in a background of free neutrons) inside which the proton superconductor forms and expands. The strong gradients in density ρ and T_c , together with the temperature dependence of H_c , lead to a broad normal-superconducting transition; there is no static equilibrium for the system to reach for at least decades, and potentially far longer [17].

The long-standing uncertainty about whether effective flux expulsion is possible in NSs has led to a major tension in the literature: microscopic arguments [3] suggest that flux expulsion is negligibly slow even for $B < H_c$, leading to a core threaded by \mathbf{B} quantised into thin flux-tubes, and yet most simulations of crustal magnetic-field evolution (e.g. [4, 5]) assume that it is *always* expelled and use a zero-field inner boundary condition. The uncertainty stems from the fact that the Meissner ‘effect’ is simply a statement about the minimum-energy equilibrium, and offers no description of the process by which the system realises this state. Recently, a novel model

that examines the gradual transition to superconductivity in the NS core was put forward [22]. The proposed mechanism is the only one to date that could realise a Meissner expulsion inside NSs on fast enough timescales to be astrophysically relevant [6], thus resolving the tension between previous theoretical work and magnetar phenomenology and modelling. As well as the case of full expulsion, it was shown that another likely outcome is a $B = 0$ shell that is broken by one or two large holes through which \mathbf{B} penetrates (see below and [22] for details). In this Letter we outline the main ideas of the model, and focus on the numerous important observational consequences of such an effective expulsion mechanism: a late-time energy injection following a supernova, delayed crustal evolution resembling the activity of some recently-discovered long-period radio sources, changes to the mature star’s rotational properties, and a revised prognosis for the detection of continuous gravitational waves from pulsars like the Crab.

The onset of superconductivity. T_c varies throughout the core of a NS, peaking at a value $\sim (3 - 7) \times 10^9 \text{ K}$ [7], which is attained only minutes after the star’s formation. The range of peak values for T_c reflects differing approaches to calculating the energy gap. Here we adopt an approximation [8] to one particular energy gap model [9], together with a ρ distribution for an equilibrium with the SLy equation of state [10], and a standard cooling prescription [11]. This gives a first thin shell of superconductivity forming at a radius of $0.79R_*$ (where R_* is the stellar radius), a temperature $T = 6.8 \times 10^9 \text{ K}$, and a stellar age of 170 seconds. The shell spreads rapidly, enveloping half of the core radius (neglecting magnetic-field effects for now) after ~ 1 day. Another important quantity for our model is H_c , which varies by a factor of ~ 5 within the core [12], but not monotonically, and also depends upon the equation of state, the nature of core

superconductivity, and the geometry of \mathbf{B} . We cannot account for all these features and retain any generality in the model, so for simplicity we approximate H_c as a constant, adopting a representative value $H_c = 5 \times 10^{14}$ G.

The production of a macroscopic $B = 0$ region in the core has typically been associated with very slow mechanisms for flux transport (e.g. [3, 13–15]), i.e. implicitly assuming that the process of rearranging \mathbf{B} , to achieve Meissner expulsion, must be secular and dissipative. For example, the estimated expulsion time for a field of characteristic lengthscale l_{char} through Ohmic decay,

$$\tau_{\text{Ohm}} = 4\pi\sigma l_{\text{char}}^2/c^2, \quad (1)$$

is of order 10^9 yr for $l_{\text{char}} = R_*$ and a typical value for the NS core's electrical conductivity σ [16]. Such slow expulsion suggests that magnetic fluxtubes thread the interior of every observed NS – even in the likely case where $B < H_c$. The nature of Meissner expulsion achieved through this process was recently quantified [17] through a comparison of the cooling and flux dissipation timescales that accounted for the gradual spreading of the superconducting shell, with the conclusion that for NSs younger than 10^6 yr, any field-free regions will likely be $\lesssim 10^3$ cm in extent.

However, the Meissner ‘effect’ is not intrinsically dissipative, so let us instead consider whether advection of field lines could, in principle, shear the field into a geometry amenable to magnetic reconnection across the nascent shell of superconductivity, thus separating the inner and outer parts of the flux distribution. In this scenario, the relevant timescale for magnetic-field rearrangement is not secular and dissipative, but rather the dynamical timescale associated with the advection of field by the fluid flow with velocity \mathbf{v} :

$$\frac{\partial \mathbf{B}}{\partial t} = \nabla \times (\mathbf{v} \times \mathbf{B}), \quad (2)$$

where $|\mathbf{v}|$ may be as large as the Alfvén speed $v_A = B/\sqrt{4\pi\rho}$, leading to a characteristic dynamical timescale

$$\tau_A = \frac{l_{\text{char}}}{v_A} = \frac{l_{\text{char}}\sqrt{4\pi\rho}}{B} = 35 l_{\text{char},6}\rho_{14}^{1/2} B_{12}^{-1} \text{ sec}, \quad (3)$$

where we have introduced the shorthand notation $X_n \equiv 10^{-n} X$ [cgs units] for any variable X , e.g. $l_{\text{char},6} = l_{\text{char}}/(10^6 \text{ cm})$. To understand how much \mathbf{B} may be advected by fluid motions before the superconducting layer expands, we compare τ_A with the cooling timescale

$$\tau_{\text{cool}} \approx 3 \times 10^6 T_9^{-6} \text{ sec}, \quad (4)$$

where we have used fiducial values for the temperature-luminosity relation and heat capacity [11]). Evaluating the previous two equations for ρ, T at the onset of superconductivity and taking $l_{\text{char},6} = B_{12} = 1$, we see that $\tau_A \sim \tau_{\text{cool}}$, indicating that the efficacy of field rearrangement depends quite sensitively on B and l_{char} at the onset of superconductivity.

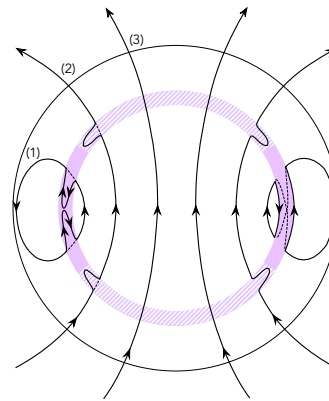


FIG. 1. Shearing and reconnection of field lines dictate the final extent of the $B = 0$ region. On the left, three field lines cross the incipient superconducting shell (thick purple band) and undergo: substantial shearing yielding an X-point geometry (1), moderate shearing (2), no shearing (3); the dashed segments show the original positions of the field lines across the shell, and the solid segments their later sheared states. On the right, field line (1) has undergone reconnection and no longer crosses the shell, whilst the latter two remain with the same geometry as on the left. The resulting superconducting shell has $B = 0$ in the solid purple regions, $B \neq 0$ throughout the striped region (the two polar ‘holes’).

Early-phase field rearrangement. The incipient shell of superconductivity will, for any realistic \mathbf{B} geometry, be crossed by field lines – i.e. the radial field B_r will be substantial. These field lines cannot just be ‘cut’ to yield a $B = 0$ shell, since radial discontinuities violate $\nabla \cdot \mathbf{B} = 0$, but they could be rearranged into an angular component by advection via a suitable fluid flow. If this results in an X-point field geometry reconnection can occur, yielding a $B = 0$ shell just under the crust-core boundary (see Fig. 1), but only if these processes are faster than the spreading of the superconducting shell.

To evaluate the reconnection process we note that the (usually efficient) mechanism of stochastic reconnection [18] is likely to be seriously inhibited in NSs [19], and so consider only the standard Sweet-Parker reconnection [20, 21], whose timescale τ_{rec} is that of Ohmic decay, equation (1). Combining this with equation (4), and using a ρ, T -dependent expression for σ [16], yields a ratio of timescales

$$\frac{\tau_{\text{rec}}}{\tau_{\text{cool}}} = 4.2 \times 10^5 \rho_{c,15}^{-3/2} \rho_{15}^3 T_{10}^{-8} l_{\text{char},1}^2. \quad (5)$$

Comparing this with the minimum lengthscale for viscous MHD motions at the onset of superconductivity [22]

$$l_{\text{char}} \approx 10^{-3} B_{12}^{-1} \text{ cm}, \quad (6)$$

shows that reconnection across the nascent shell of superconductivity is ineffective if $B \lesssim 10^{12}$ G. Furthermore, demanding that field lines be advected to bring them into an X-point geometry, a distance of $\sim 10^6$ cm (see Fig. 1)

also leads – from equations (3) and (4) – to the same lower bound on B , below which we do not expect any dynamical-timescale Meissner effect. We also know that for $B > H_c$ field expulsion is not energetically favourable. Together, then, a Meissner state is *possible* only when

$$10^{12} \text{ G} \lesssim B \lesssim 5 \times 10^{14} \text{ G}. \quad (7)$$

Even within this range, the field geometry need not be conducive to complete reconnection. In axisymmetry, shearing and reconnection of a dipolar field at the incipient shell can instead lead to a broken $B = 0$ superconducting shell, pierced with field lines through either two roughly cylindrical $B \neq 0$ holes (one at each pole), or one equatorial band; see Fig. 1. The size of these $B \neq 0$ regions in the shell may be calculated from conservation of magnetic flux $\mathfrak{F} \propto BR^2$ and the requirement that $B \leq H_c$; the result is holes whose cross-sectional area is proportional to B . Whether or not this $B = 0$ shell is complete, however, there must always be an inner trapped core of magnetic field that will be compressed until it reaches $B = H_c$. Magnetic flux conservation then yields an estimate of the final radius R_{in} of this inner core:

$$R_{\text{in}} \approx R_* \sqrt{B/H_c}. \quad (8)$$

Energy release at onset of superconductivity. The kind of shearing motion needed to bring a large-scale dipole field into an X-point geometry can be seen from Fig. 1 to result in an approximate doubling of a typical field line’s length and so, assuming the internal field is approximately uniform, also doubling the magnetic energy; this is backed up by detailed calculations [22]. But a partial or complete reconnection event, needed to produce a $B = 0$ shell, will return \mathbf{B} to a less-sheared, lower-energy configuration. Thus, realising the Meissner effect involves a sudden energy release comparable in magnitude to that of the pre-condensation magnetic energy, which can be as large as 5×10^{46} erg.

This reconnection energy release in the core will cause local heating but also drive the shaking of field lines through the still-molten crust, out to the magnetosphere and beyond. If this complex process of transferring reconnection energy into a detectable signal is radiatively efficient, the reconnection event could ultimately be seen as a peculiar transient, possibly involving delayed energy injection into the supernova remnant. Given the vast zoo of optical transients [23], it is possible such signals may have already been detected. Alternatively, the reconnection event might be more readily identifiable if a binary neutron star merger produces a massive magnetized neutron star remnant: a cleaner environment for signals to transit. Many short gamma-ray bursts exhibit X-ray extended emission (lasting $\sim 10^2 - 10^3$ s), whose physical origin is uncertain and requires delayed energy injection [24]. Secure association of such signals would be profoundly important, as its timing would constrain the maximum value of the T_c and therefore the gap model.

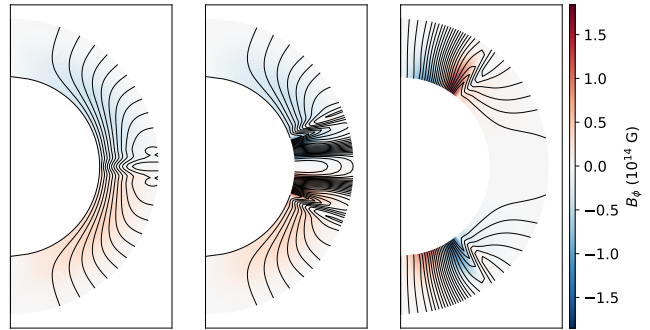


FIG. 2. Magnetic field in the crust (here scaled up in thickness by a factor of 8 for clarity) after 0.1 Myr of evolution, where the inner boundary at the base of the crust is: $B = 0$ everywhere (left), field lines penetrating into the core in a band around the equator (middle), field lines penetrate into the core in two polar holes (right). Poloidal field lines are in black, toroidal field magnitude is shown with the colourscale.

Crustal field evolution. The evolution of \mathbf{B} in a NS crust is described by the equation [25]

$$\frac{\partial \mathbf{B}}{\partial t} = -\frac{1}{4\pi} \nabla \times \left(\frac{c}{\rho_e} (\nabla \times \mathbf{B}) \times \mathbf{B} - \frac{c^2}{\sigma} \nabla \times \mathbf{B} \right) \quad (9)$$

where the first term on the right-hand side is Hall drift, the second Ohmic decay, and ρ_e is the charge density.

In the absence of our model for the Meissner effect, B will penetrate from the crust into the core, which should be incorporated as a $B \neq 0$ inner boundary condition when evolving equation (9). The result is a slowly evolving \mathbf{B} without any particularly dramatic features [26]. By contrast, the $B = 0$ inner boundary condition that is usually employed results, for young NSs ($10^3 - 10^4$ yr) with crustal fields $\gtrsim 10^{13}$ G, in an active Hall drift that produces local patches of intense field; conversely, for older sources the Hall effect saturates [27] and eventually Ohmic decay dominates, smoothing out small-scale features and weakening the field (see e.g. [5]). This fits with the theoretical picture of canonical magnetars as young and highly magnetised NSs whose activity is powered by crustal magnetic-field evolution. The dynamical Meissner effect we discuss here is the first scenario to provide a physical justification for this $B = 0$ boundary condition, which is crucial to produce evolutions that resemble magnetars. However, it also allows for other, equally viable, inner boundary conditions, where the complete $B = 0$ shell is broken by regions threaded by field lines: either an equatorial band, or two polar holes. We have performed evolutions for these new ‘hole’ boundary conditions, utilising a code well tested in earlier applications [28], and taking an initially simple poloidal field. Figure 2 shows sample results after 0.1 Myr of evolution. With the usual $B = 0$ inner boundary (left-hand panel), the crustal field at this late stage has settled into a quasi-stationary state,

with no sharp features, and is relatively weak: the maximum value of the toroidal field $B_\phi^{\max} = 4 \times 10^{13}$ G. By contrast, the simulation with $B = 0$ around the poles but $B \neq 0$ in an equatorial band (middle panel) is still very dynamic at this age, displaying sharp features in the poloidal field lines and $B_\phi^{\max} = 1.6 \times 10^{14}$ G close to the transition region between the $B = 0$ and $B \neq 0$ surfaces. Above this region, at the top of the crust, small closed magnetic-field loops are progressively pushed out of the star. All these features, which are shared with the corresponding simulation featuring polar $B \neq 0$ holes (right-hand panel), are qualitatively new and suggest the existence of a class of NS that becomes more active at ~ 100 times the age of conventional magnetars.

In fact, such qualitatively different ‘old magnetars’ may have already been observed. The recent discoveries of very long-period intermittent radio sources [29–31] and a repeating fast radio burst (FRB) source in a globular cluster [32], largely unexpected by theorists, are plausibly explained by the delayed activation of highly magnetised older NSs. Yet, identifying a mechanism for this re-activation had been a problem [33] – to which our work offers a natural solution. In addition, standard accretion models for formation of long neutron stars in some high-mass X-ray binaries require sustained magnetar-like fields for $\gg 10^4$ yr [34].

Continuous gravitational wave emission. Recent studies on the non-detection of continuous gravitational waves from various pulsars have put some stringent and physically-interesting bounds on the ellipticity ϵ [35]. For example, the Crab pulsar has $\epsilon \lesssim 3 \times 10^{-5}$ [36], and this limit will continue to drop with advances in gravitational-wave interferometry. The Crab’s inferred dipole surface magnetic field $B_{\text{dip}} = 4 \times 10^{12}$ G. If the primary source of distortion is an average interior field \bar{B}_{int} threading the entire core, ellipticity calculations for superconducting NSs [37] allow us to infer that

$$\bar{B}_{\text{int}} \lesssim 10^{15} \text{ G} \approx 300 B_{\text{dip}}. \quad (10)$$

Alternatively, we can invert the calculation to assess the prospects for a future gravitational-wave detection from the Crab, and how the Meissner effect alters this prognosis. A typical NS could plausibly [38] harbour a field with $\bar{B}_{\text{int}} \gg B_{\text{dip}}$; let us take, for example, $\bar{B}_{\text{int}} = 20 B_{\text{dip}}$ for the Crab, close to typical magnetar values. If the Meissner effect has expelled the field from a complete shell of the star, it will cease once an inner core of $\bar{B} = H_c$, $R_{\text{in}} \approx 0.4 R_*$ (see equation (8)) has been formed. However, the ellipticity for a superconducting core scales as $\epsilon \propto \bar{B} R_{\text{in}}^3$, so although \bar{B} has been increased substantially through flux compression, the overall effect on ϵ is dominated by the decrease in R_{core} . As a result, the ellipticity for the Meissner-expelled model ϵ_M is substantially lower than that of the non-Meissner model ϵ_{nM} (i.e.

where field lines thread the entire core):

$$\epsilon_M \approx 3 \times 10^{-7}, \epsilon_{nM} \approx 2 \times 10^{-6}. \quad (11)$$

In this scenario, if the Crab hosts a Meissner-expelled region, we would expect weak gravitational-wave emission, but notable magnetar-like activity (given that a crustal field of strength $20 B_{\text{dip}}$ would have evolved substantially over the lifetime of the Crab). The latter has not been seen from the Crab, despite over fifty years of monitoring, leading us to conclude that *if* the Crab has a strong \bar{B}_{int} it must thread the entire core. Its associated gravitational-wave signal would then be below the sensitivity of current instruments by a factor of ~ 10 , but could plausibly be seen by next-generation detectors.

Rotational dynamics. Most models of NS rotation (in contrast with magnetar modelling) assume a continuous \mathbf{B} threading the core and connecting it to the crust. This provides fast electromagnetic coupling between all charged core components and the crust, irrespective of whether the protons are superconducting, which justifies treating them as being in co-rotation. If the neutrons are normal, they will also be strongly coupled: either near-instantaneously via the strong interaction (for normal protons), or due to particle collisions (for superconducting protons) – still a relatively rapid process compared with most other timescales of interest, e.g. spin-down (see [1, 39] and references therein).

The presence of a macroscopic $B = 0$ region could drastically change this picture. Spin-down is then likely achieved by the formation of a viscous crust-core boundary layer. The associated Ekman flow should reduce the coupling timescale compared to that of viscous diffusion, although realistic modelling remains challenging. It is conceivable that a magnetically-decoupled region (the $B = 0$ shell and, for full Meissner expulsion, the inner $B \neq 0$ core too) would deviate from ‘rigid’ co-rotation with the crust (cf. [40, 41] for core superrotation in other setups); this problem deserves a careful treatment (including, e.g., the various interfaces) to assess whether it could lead to a long-lived rotational lag, or affect the response to fast spin changes, like pulsar glitches.

Superfluid core neutrons rotate by forming vortices, which couple to the charged component via mutual friction. In the presence of superconducting protons the dominant coupling mechanism is then due to vortex magnetisation, leading to electron-vortex relaxation timescales of $\sim 1 - 10$ sec [39]. Thus the core superfluid maintains differential rotation but is close to corotation and spins down with the local charged component. Interactions between vortices and fluxtubes have been extensively studied in the literature (e.g. [42]), mostly in relation to mode damping, arguments against long-period neutron star precession [43], and the angular momentum reservoir available to generate large glitches as in the Vela pulsar [44]. These results could change drastically in a $B = 0$ region, since fluxtubes will no longer co-exist with

neutron vortices there, and so should be re-evaluated for the different Meissner scenarios discussed here. For example, in the case of a $B \neq 0$ equatorial band vortices could naturally pin to a different number of fluxtubes depending on the pulsar, giving rise to different glitch signatures [45]. By contrast, in the fully Meissner-expelled or polar-hole case, vortices might not be pinned at all, resolving contradictions with long-period precession and some glitch models [46, 47].

Outlook. The existence of a field-free region in a NS core is crucial to drive significant crustal field evolution within 10^4 yr; without any mechanism for field expulsion, the currently accepted paradigm for magnetar activity would be seriously undermined. The dynamical Meissner effect explored here (see [22] for a full discussion) provides the first theoretical support for this crucial, yet unquestioned, assumption. It also leads us to a number of predictions for how one could actually observe the Meissner effect, including through an energy injection in the late supernova phase, and through the rotational behaviour and gravitational-wave emission of mature NSs.

The Meissner model discussed here also implies that there are three different observational incarnations of a highly magnetised NS. Only one of these is a classical magnetar: the case of full Meissner expulsion from the outer core, which we argue implies their internal fields must be in the range $0.01 \lesssim B_{14} \lesssim H_{c,14} \approx 5$. Interestingly, this is not very different from the range of B_{dip} values for known magnetars [48],[49], $0.06 \lesssim B_{\text{dip},14} < 8$. We predict that NSs born with $\bar{B}_{\text{int}} > H_c$ will never display magnetar activity, although their substantial magnetic distortions could make them promising sources of gravitational waves. Finally, NSs possessing a partially Meissner-expelled shell with ‘holes’ should become active once substantially older than normal magnetars.

This work was supported by computational time granted from the National Infrastructures for Research and Technology S.A. (GRNET S.A.) in the National HPC facility-ARIS-under project ID pr015026/simnstar. We thank Bryn Haskell, Mike J. Moss and Brad Cenko for helpful discussions on some of these topics. Z.W. acknowledges support by NASA under award number 80GSFC21M0002. D.A. acknowledges support from a UKRI (STFC/EPSC) fellowship (EP/T017325/1). This work has made use of the NASA Astrophysics Data System.

* samuel.lander@uea.ac.uk

- [1] B. Haskell and A. Sedrakian, in *Astrophysics and Space Science Library*, Astrophysics and Space Science Library, Vol. 457, edited by L. Rezzolla, P. Pizzochero, D. I. Jones, N. Rea, and I. Vidaña (2018) p. 401.
- [2] M. Tinkham, *Introduction to superconductivity* (Courier Corporation, 2004).

- [3] G. Baym, C. Pethick, and D. Pines, *Nature* **224**, 673 (1969).
- [4] R. Hollerbach and G. Rüdiger, *MNRAS* **337**, 216 (2002).
- [5] J. A. Pons and U. Geppert, *A&A* **470**, 303 (2007).
- [6] Previous work predicted it would take $\gtrsim 10^6$ yr.
- [7] W. C. G. Ho, K. G. Elshamouty, C. O. Heinke, and A. Y. Potekhin, *PRC* **91**, 015806 (2015).
- [8] W. C. G. Ho, K. Glampedakis, and N. Andersson, *MNRAS* **422**, 2632 (2012).
- [9] J. M. C. Chen, J. W. Clark, R. D. Davé, and V. V. Khodel, *Nuc. Phys. A* **555**, 59 (1993).
- [10] F. Douchin and P. Haensel, *A&A* **380**, 151 (2001).
- [11] D. Page, U. Geppert, and F. Weber, *Nuc. Phys. A* **777**, 497 (2006).
- [12] K. Glampedakis, N. Andersson, and L. Samuelsson, *MNRAS* **410**, 805 (2011).
- [13] P. B. Jones, *Mon. Not. Roy. Astron. Soc.* **253**, 279 (1991).
- [14] V. V. Kocharovskiy, V. V. Kocharovskiy, and V. A. Kukushkin, *Radiophysics and Quantum Electronics* **39**, 18 (1996).
- [15] V. Graber, N. Andersson, K. Glampedakis, and S. K. Lander, *Mon. Not. Roy. Astron. Soc.* **453**, 671 (2015).
- [16] G. Baym, C. Pethick, and D. Pines, *Nature* **224**, 674 (1969).
- [17] W. C. G. Ho, N. Andersson, and V. Graber, *Phys. Rev. C* **96**, 065801 (2017).
- [18] A. Lazarian and E. T. Vishniac, *Astrophys. J.* **517**, 700 (1999).
- [19] S. K. Lander, *MNRAS* **507**, L36 (2021).
- [20] P. A. Sweet, in *Electromagnetic Phenomena in Cosmical Physics*, Vol. 6, edited by B. Lehnert (1958) p. 123.
- [21] E. N. Parker, *J. Geophys. Res.* **62**, 509 (1957).
- [22] S. K. Lander, *MNRAS*, accepted <https://doi.org/10.1093/mnras/stae2453> (2024).
- [23] M. R. Drout, R. Chornock, A. M. Soderberg, N. E. Sanders, R. McKinnon, A. Rest, R. J. Foley, D. Milisavljevic, R. Margutti, E. Berger, M. Calkins, W. Fong, S. Gezari, M. E. Huber, E. Kankare, R. P. Kirshner, C. Leibler, R. Lunnan, S. Mattila, G. H. Marion, G. Narayan, A. G. Riess, K. C. Roth, D. Scolnic, S. J. Smartt, J. L. Tonry, W. S. Burgett, K. C. Chambers, K. W. Hodapp, R. Jedicke, N. Kaiser, E. A. Magnier, N. Metcalfe, J. S. Morgan, P. A. Price, and C. Waters, *Astrophys. J.* **794**, 23 (2014), arXiv:1405.3668 [astro-ph.HE].
- [24] Y. Kaneko, Z. F. Bostancı, E. Göğüs, and L. Lin, *Mon. Not. Roy. Astron. Soc.* **452**, 824 (2015), arXiv:1506.05899 [astro-ph.HE].
- [25] P. Goldreich and A. Reisenegger, *Astrophys. J.* **395**, 250 (1992).
- [26] D. Viganò, N. Rea, J. A. Pons, R. Perna, D. N. Aguilera, and J. A. Miralles, *Mon. Not. Roy. Astron. Soc.* **434**, 123 (2013).
- [27] K. N. Gourgouliatos and A. Cumming, *Phys. Rev. Lett.* **112**, 171101 (2014).
- [28] K. N. Gourgouliatos and S. K. Lander, *Mon. Not. Roy. Astron. Soc.* **506**, 3578 (2021).
- [29] M. Caleb, I. Heywood, K. Rajwade, M. Malenta, B. Stappers, E. Barr, W. Chen, V. Morello, S. Sanidas, J. v. d. Eijnden, M. Kramer, D. Buckley, J. Brink, S. E. Motta, P. Woudt, P. Weltevrede, F. Jankowski, M. Surnis, S. Buchner, M. C. Bezuidenhout, L. N. Driessen, and R. Fender, *Nature Astronomy* **6**, 828

- (2022), arXiv:2206.01346 [astro-ph].
- [30] N. Hurley-Walker, T. J. Galvin, S. W. Duchesne, X. Zhang, J. Morgan, P. J. Hancock, T. An, T. M. O. Franzen, G. Heald, K. Ross, T. Vernstrom, G. E. Anderson, B. M. Gaensler, M. Johnston-Hollitt, D. L. Kaplan, C. J. Riseley, S. J. Tingay, and M. Walker, *Publications of the Astronomical Society of Australia* **39**, e035 (2022).
- [31] F. A. Dong, T. Clarke, A. P. Curtin, A. Kumar, I. Stairs, S. Chatterjee, A. M. Cook, E. Fonseca, B. M. Gaensler, J. W. T. Hessels, V. M. Kaspi, M. Lazda, K. W. Masui, J. W. McKee, B. W. Meyers, A. B. Pearlman, S. M. Ransom, P. Scholz, K. Shin, K. M. Smith, and C. M. Tan, arXiv e-prints, arXiv:2407.07480 (2024), arXiv:2407.07480 [astro-ph.HE].
- [32] F. Kirsten, B. Marcote, K. Nimmo, J. W. T. Hessels, M. Bhardwaj, S. P. Tendulkar, A. Keimpema, J. Yang, M. P. Snelders, P. Scholz, A. B. Pearlman, C. J. Law, W. M. Peters, M. Giroletti, Z. Paragi, C. Bassa, D. M. Hewitt, U. Bach, V. Bezrukovs, M. Burgay, S. T. Buttaccio, J. E. Conway, A. Corongiu, R. Feiler, O. Forssén, M. P. Gawroński, R. Karuppusamy, M. A. Kharinov, M. Lindqvist, G. Maccaferri, A. Melnikov, O. S. Ould-Boukattine, A. Possenti, G. Surcis, N. Wang, J. Yuan, K. Aggarwal, R. Anna-Thomas, G. C. Bower, R. Blaauw, S. Burke-Spolaor, T. Cassanelli, T. E. Clarke, E. Fonseca, B. M. Gaensler, A. Gopinath, V. M. Kaspi, N. Kasim, T. J. W. Lazio, C. Leung, D. Z. Li, H. H. Lin, K. W. Masui, R. Mckinven, D. Michilli, A. G. Mikhailov, C. Ng, A. Orbidans, U. L. Pen, E. Petroff, M. Rahman, S. M. Ransom, K. Shin, K. M. Smith, I. H. Stairs, and W. Vlemmings, *Nature* **602**, 585 (2022), arXiv:2105.11445 [astro-ph.HE].
- [33] P. Beniamini, Z. Wadiasingh, J. Hare, K. M. Rajwade, G. Younes, and A. J. van der Horst, *Monthly Notices of the Royal Astronomical Society* **520**, 1872 (2023).
- [34] X. D. Li and E. P. J. van den Heuvel, *Astrophys. J. Lett.* **513**, L45 (1999), arXiv:astro-ph/9901084 [astro-ph].
- [35] B. Abbott, R. Abbott, R. Adhikari, and et al., *Astrophys. J. Lett.* **683**, L45 (2008).
- [36] R. Abbott, T. D. Abbott, F. Acernese, K. Ackley, and et al, *Astrophys. J.* **932**, 133 (2022).
- [37] S. K. Lander, *Mon. Not. Roy. Astron. Soc.* **437**, 424 (2014).
- [38] A. P. Igoshev, K. N. Gourgouliatos, R. Hollerbach, and T. S. Wood, *Astrophys. J.* **909**, 101 (2021).
- [39] M. A. Alpar, S. A. Langer, and J. A. Sauls, *Astrophys. J.* **282**, 533 (1984).
- [40] A. Melatos, *Astrophys. J.* **761**, 32 (2012).
- [41] K. Glampedakis and P. D. Lasky, *Mon. Not. Roy. Astron. Soc.* **450**, 1638 (2015).
- [42] A. Sourie and N. Chamel, *Mon. Not. Roy. Astron. Soc.* **493**, 382 (2020).
- [43] B. Link, *Phys. Rev. Lett.* **91**, 101101 (2003).
- [44] N. Andersson, K. Glampedakis, W. C. G. Ho, and C. M. Espinoza, *Phys. Rev. Lett.* **109**, 241103 (2012).
- [45] A. Sourie and N. Chamel, *Mon. Not. Roy. Astron. Soc.* **493**, L98 (2020).
- [46] B. Link, *Astron. Astrophys.* **458**, 881 (2006).
- [47] B. Haskell, P. M. Pizzochero, and S. Seveso, *Astrophys. J. Lett.* **764**, L25 (2013).
- [48] N. Rea, G. L. Israel, J. A. Pons, R. Turolla, D. Viganò, S. Zane, P. Esposito, R. Perna, A. Papitto, G. Terreran, A. Tiengo, D. Salvetti, J. M. Girart, A. Palau, A. Possenti, M. Burgay, E. Göğüş, G. A. Caliendo, C. Kouveliotou, D. Götz, R. P. Mignani, E. Ratti, and L. Stella, *Astrophys. J.* **770**, 65 (2013).
- [49] The widely-quoted value of 2×10^{15} G for SGR 1806-20 was inferred during the epoch of its giant flare, with a correspondingly enhanced spindown; now its rotation has stabilised, leading to a new and more reliable estimate of 7.7×10^{14} G [50].
- [50] G. Younes, M. G. Baring, C. Kouveliotou, A. Harding, S. Donovan, E. Göğüş, V. Kaspi, and J. Granot, *Astrophys. J.* **851**, 17 (2017).